Development of a Cosmic Ray Telescope

Author: Bernardo D'Almeida M. do Rosário[1] and
Supervisor: Pedro Jorge dos Santos Assis, PhD[1]

[1] *Instituto Superior Técnico, LIP*

(Dated: April 26, 2016)

Motivation

The field of cosmic rays and particle is currently pushing the fringe of our knowledge. Trying to prove the soundness of the standard model while at the same time trying to figure out how our universe came into existence. It challenges our concepts and imagination yet it seems to out of reach and disconnected from the common people. It is common to perceive that studies in the field of particle physics are only possible with complex and vastly expensive equipment while supervised by hundreds of highly qualified scientists and engineers. Yet that paradigm is changing. With few resources it, already, is possible to build real instruments that can detect and make measurements of actual elementary particles, using as a base, components used on large scale particle detectors.

The goal of this project is to create such a detector. It must be built using few resources in order to be relatively cheap, safe to handle so that there is no danger for the users and robust enough that it will not break easily. With this characteristics it opens the possibility to study particle physics to an academic level and bringing students closer to this field of research. Providing a teaching tool, that is an asset to the formation of students that so far is not available.

1. COMPACT MUON DETECTOR

The purpose of this thesis is the development and study of compact muon detector prototype directed for academic purposes, that can be controlled by students on their own and even be used within high school lessons. This project was originally inspired by the CosMOS [1] (Cosmic Muon Observer) experiment developed by DESY and other partner institutes within Netzwerk Teilchenwelt. This experiment is composed by a scintillation counter and a data acquisition card.

The CMuD prototype was developed in LIP, *Laboratório de Instrumentação e Física Experimental de Partículas* where the project was envisioned, developed, assembled and tested.

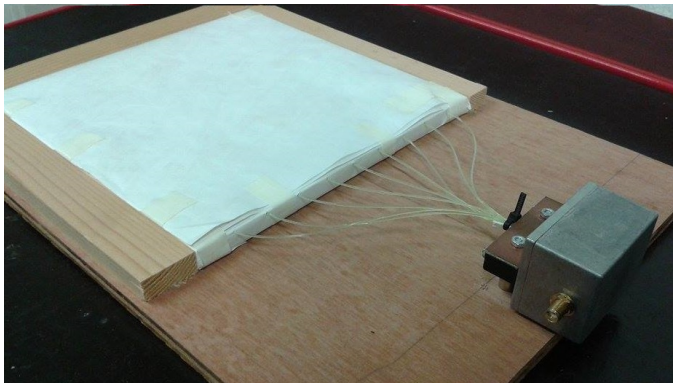

Figure 1: CMuD prototype.

The CMuD is compounded three main elements:

- Scintillator
- WLS fiber
- MPPC - Silicon Photomultiplier

The CMuD uses a plastic scintillator tile with $20 \times 20 \times 1.25\ cm^3$. Nine wavelength shifting fibers, with 1 mm of diameter are placed in parallel shallow grooves along the scintillator, separated 2 cm from each other. The detector is wrapped in a double layer of Tyvek reflective material to prevent the light from escaping it. The WLS fibers are used to collect and guide the photons generated by the scintillator to a multi-pixel photon counter (MPPC), while at the same time changing its wavelength to better match the photo-detector response peak. A plastic piece with grooves provides the mechanical alignment of the fibers. The metal box seen in figure 1 houses the MPPC along with the front-end electronics that the decouples the power supply from the signal generated. The first prototype was built using spare parts available at LIP, which strongly conditioned the selection of the components.

1.1. Scintillator EJ-200 & Y-11(200) Wavelength Shifting Fibers

This project used the combination of the plastic scintillator, EJ-200 from the *Eljem Technologies*, with the multi cladding WLS fibers, Y-11(200) from Kuraray.

The EJ-200 scintillator combines the two properties of long optical attenuation length and fast timing, and is therefore particularly useful for time-of-flight systems using scintillators greater than one meter long. It combines long attenuation length, high light output, signal uniformity and an emission spectrum well matched to the common photomultipliers.

The Y11-200 are a multi cladding fiber, which mean they are compounded by three layers of different materials. The refractive index is highest in the core material and smallest in the exterior layer. This helps increasing the light yield and trapping efficiency of the fiber.

1.2. Silicon Photomultiplier - MPPC Hamamatsu S12572-50P

The silicon photomultiplier's low price, compact size and robustness made it ideal for the purposes of this project. Besides, the MPPC has the advantage of requiring low voltages for operation which protects students from exposures to high-voltage sources. The multi-pixel photon counter S12572-50P has $3 \times 3\ mm^2$ area with 3600 individual cells with a pixel pitch of 50 μm and it uses an breakdown voltage of $\sim$ 64.15 V. Such voltage can be generated from a 5 V input using a DC-DC converter, making it possible to make the detector portable. The major downsides of this device resides in its gain variation with temperature and relatively high noise which makes the separation between signal and noise quite challenging.

2. SIGNAL ESTIMATE

With the key elements of the CMuD defined it is now possible to make a crude estimation of the signal a muon would generate. This signal represents the number of photoelectrons (phe) that will result after all the steps, from the photons creation to its translation to an electrical signal, are completed. With this estimate it will be possible to predict the order of magnitude of the threshold that should be applied to detect these particles. The calculation of the signal takes into account five separate processes: the energy deposition in the scintillator

by the ionizing particle, the conversion of that energy into photons, the collection of those photons by the WLS fibers, the re-emission of the photons in a new wavelength inside the fibers and the detection of these photons in the silicon photomultiplier. The signal, N_{phe}, is the product of the number of photons generated, N_γ by the collection efficiency , ε_{coll}, trapping efficiency, ε_{trap} and the SiPM photon detection efficiency, ε_{PDE} (see equation 1).

$$N_{phe} \;=\; N_\gamma \; \varepsilon_{coll} \; \varepsilon_{trap} \; \varepsilon_{PDE} \qquad (1)$$

2.1. Energy Deposition

When a muon crosses a scintillator it transfers some of its energy to it. This energy exchange happens primarily through ionization and atomic excitation. This energy is used to promote electrons to excited states and as they return to a more stable orbitals, photons are emitted. Therefore, in order to estimate the number of photons generated by a passing muon it is necessary to calculate the energy this particle transfers to the scintillator.

The mean rate of energy loss (stopping power) per distance traveled due to ionization and atomic excitation, expressed in MeV $g^{-1}cm^2$ is given by the *Bethe-Bloch* equation.[2][3]

The particle energy loss by ionization is relatively independent of the medium, only with a factor $\frac{Z}{A}$ to represent its influence, which is also constant for many elements. Therefore, independently of the material, there is a minimum energy loss which corresponds to the so called minimum ionizing particle (MIP). The energy deposited will increase slightly for particles with higher energies but since cosmic muons, as most relativistics particles, are essentially MIPs it is possible to estimate the mean rate of energy loss in the scintillator.

$$\frac{1}{\rho}\Big\langle\frac{dE}{dx}\Big\rangle_C \approx 2 \;\; MeV/g/cm^2 \qquad (2)$$

Integrating equation along the particles path and adding the density of the EJ-200 scintillator we obtain:

$$E_{loss} = 2\,\rho\,\frac{a}{\cos\phi}. \qquad (3)$$

Since cosmic muons are the result of complex interaction with the atmosphere the incidence angle at which these particles traverse the scintillator is not fixed. The muon angular distribution has a dependence of $\cos^2\phi$ in relation to the zenith[4]. Considering $\phi = 0$ it the most probable incidence angle, the energy deposited can be calculated.

$$E_{loss} = 2.56 \; MeV. \qquad (4)$$

2.2. Light Yield

The scintillation efficiency of the conversion of excitation energy to photons is an intrinsic characteristic of the scintillator. The light yield of the EJ-200 is of 10000 photons for each MeV of deposited energy. Therefore, the light yield is then given by:

$$N_\gamma \approx 25\,600 \;\; photons. \qquad (5)$$

2.3. Collection Efficiency

A rough approximation of the collection efficiency was performed by considering the portion of photons that reach the scintillator's top surface where the fibers are placed. We assumed that all photons are generated isotropically along the muon path. It was considered that the photons only have

two possible paths to reach the top surface, directly, when the photons are emitted with the direction of the top surface, or indirectly, when they are directed at the bottom surface and are reflected to the top surface. The fraction of photons that are directed to the top and bottom surface is approximated by the ratio of the surface areas by total area of the scintillator.

$$\Gamma_{top} = \frac{A_S}{A_T} + \frac{A_S}{A_T} R \approx 0.84\% \quad (6)$$

From the photons that reach the top surface, only the ones that reach the surface covered by the WLS fibers are collected. If the percentage of photons collected by the fibers is proportional to the area they occupy in the top surface, the collection efficiency can be calculated by:

$$\varepsilon_{coll} \approx \Gamma_{top} \frac{A_{fib}}{A_T} \approx 3.8\% \quad (7)$$

2.4. Trapping Efficiency

The purpose of WLS fibers is to absorb the photons that enter the fibers and then emit a new photon in a new wavelength, that better matches the efficiency peak of the SiPM. As a result of the isotropic emission of these photons, not all photons are collected by the fibers. The trapping efficiency of these photons is an intrinsic characteristic of the WLS fiber that depend only of the refractive index of the materials of each layer.

$$\varepsilon_{trap} = 5.4\%. \quad (8)$$

2.5. Photon Detection Efficiency

The photon detection efficiency depends on three parameters, them being: the fill form of the silicon, a geometrical factor that depends on the active area in respect to the total area of the device, the quantum efficiency that is the probability of a photon to generate a charge carrier, which by itself depends on the photon wavelength, and finally the probability that this carrier generates an avalanche which depends on the overvoltage. The PDE considered corresponds to the efficiency peak of the photo-detector with an overvoltage of 3.5 V.

$$\varepsilon_{PDE} = 0.35 \quad (9)$$

2.6. Signal

Now we have all the information necessary to estimate the average signal a muon will produce. With the number of photons generated and the efficiency of all the respective steps onto the electrical signal. These factors can now be substituted in equation 1 to obtain:

$$Signal = 25\,600 * 0.038 * 0.054 * 0.35 \approx 18\, ph.e \quad (10)$$

3. SILICON PHOTOMULTIPLIER STUDY

The silicon photomultiplier consists of an array of APD cells, each operated in Geiger-Mode. Electronically speaking, the cells of the silicon photomultiplier are connected in parallel, sharing the same bias voltage applied to the whole SiPM. If the voltage across the APD becomes larger than the intrinsic breakdown voltage of the diode, the energy will be high enough to accelerate electron-hole pairs, created by a triggering photon or thermal noise, across the junction. The current is generated leads to a voltage increase at the quenching

resistor, R_q. Consequently, the voltage across the diode decreases and the electric field is not strong enough to accelerate charge carriers through the junction anymore. Thus the avalanche process is 'quenched'. Because no current flows through the diode at this time, the voltage at the diode increases again, reaching the bias voltage and the process restarts.

Having explained the basic working principle of a single SiPM cell it is now possible to describe the complete SiPM as an array of Geiger Mode - APDs. In this section, some of the the SiPMs characteristics were studied. When talking about the SiPM response it is important to know that its output signal has well defined amplitudes which is shown in 2. This height depends on the number of cells that discharged and of the gain produced in the avalanche which itself depends on the applied bias voltage. The smallest pulse a SiPM is able to output is referred to as a one photo-electron equivalent (1 ph.e.). Larger pulses are integer multiples of this signal with some uncertainty due to statistical processes in the cell.

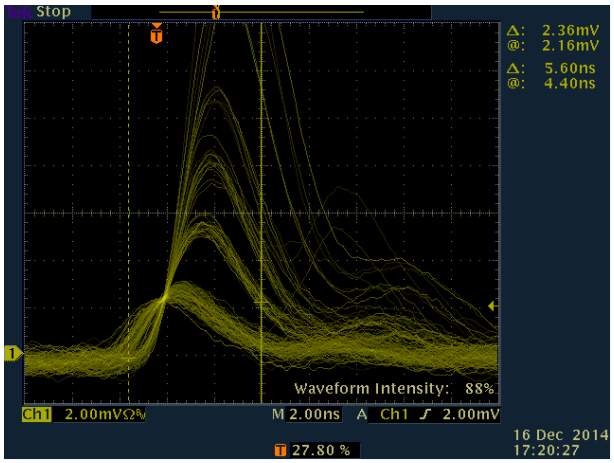

Figure 2: MPPC Hamamatsu S12572-50P The pulses have well defined amplitudes that multiple of the number of APD's that discharged.

3.1. Gain Variation

Gain is the internal amplification of the SiPM expressed as the average number of charge carriers produced from a single original pair electron-hole. Its gain depends on the overvoltage voltage applied. If the electric field in the p-n junction is higher when an electron-hole pair is generated the acceleration is also higher, producing a larger number of carriers in the avalanche.

Using the oscilloscope, three pulses were acquired for each overvoltage value. The charge was calculated by integrating the pulse. The resulting charge was divided by the gain of the amplifier using the conversion factor and expressed in number of electrons. The result is the number of electrons that were generated in the avalanche inside the SiPM cell. The data was plotted as a function of the overvoltage in figure 3. The gain of the MPPC shows a linear relation with the overvoltage with a slope 5.28×10^5.

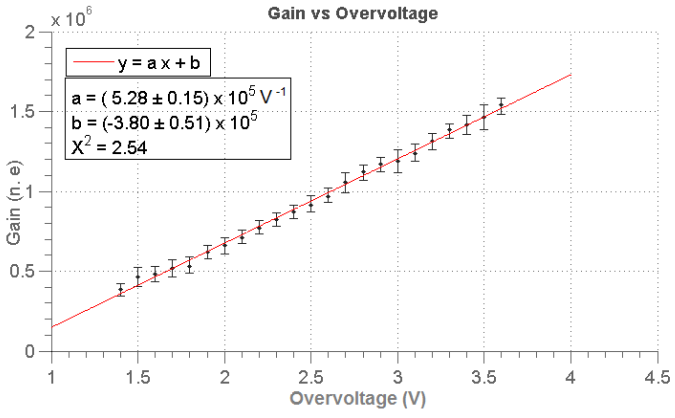

Figure 3: Plot of the SiPM gain as a function of the overvoltage and corresponding linear fit.

3.2. Dark Current & Photo-electron determination

In the absence of photons, the thermal motion of electrons-holes inside the depletion region can be enough for it to jump to the conduction band and thus triggering a discharge inside that cell. The events created by this process contribute to the noise of the photo-detector. This random process occurs independently inside each cell and it's rate depends only of the temperature and the size of the depletion region of the cell. Therefore there is a fixed rate of false events always present in the SiPM. This rate is called dark current, since it is the signal that the SiPM produces even in the absence of light.

The determination of a photo-electron is important to define a scale that is independent of the amplification or circuit used to measure the signal.

In figure 4 is represented the data acquired corresponding to the dark current. In the lower thresholds it is possible to observe a few plateaus that correspond to the voltage gap between each ph.e. As the threshold increases the steps blend with the main curve and disappear. This is because there is always some uncertainty in the signal resulting from a discharge of a cell.

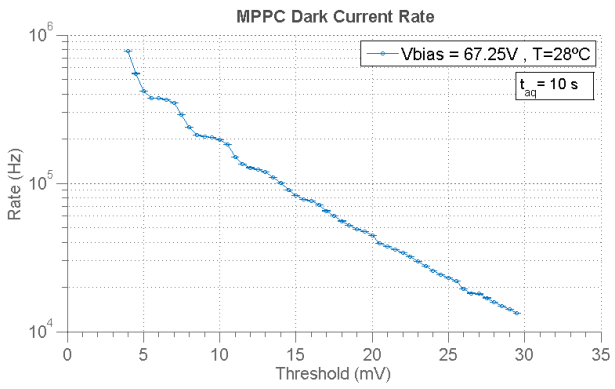

Figure 4: Plot of the dark current rate in logarithmic scale.

To determine the ph.e voltage, the threshold distance between each visible step was measured. To determine the photo-electron voltage the first four valleys were used and the distances averaged to obtain:

$$1\,ph.e = 3.3 \pm 0.1 mV. \tag{11}$$

This means that the amplitude of the output signal increases about 3.3 mV for each ph.e, i.e., cell discharge. The threshold voltage will be expressed in ph.e scale using this scaling factor.

The dark current appears to follow a Poisson distribution and decrease exponentially. To estimate the rate at which it decreases a fit was attempted. The data selected was plotted and fitted in figure 5.

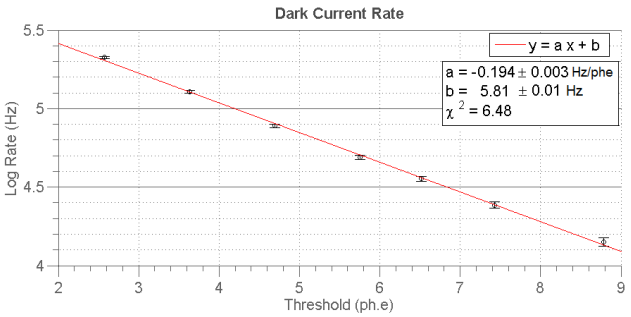

Figure 5: Linear fit of the dark current rate in logarithmic scale versus threshold in ph.e.

The fit gives the approximate rate at which the logarithmic dark current rate decreases with the threshold in photo-electrons.

$$\log_{10}[\,R_{DC}(T_h)\,] = -0.194\,T_h + 5.81 \tag{12}$$

4. CMUD

In this chapter it will determined some of the characteristics of the CMuD in different functioning modes. First the CMuD was tested by itself and

its efficiency and purity were determined. These characteristics were also measured with two CMuD working in coincidence and in self-coincidence. The self-coincidence mode was obtained by dividing the 9 WLS fibers, from one detector, by two different MPPC.

This section will be divided in three subsection each corresponding to a different setup. The efficiency and purity were measured for each one of these setups. In the first the instance the characteristics intrinsic to the CMuD were studied. Then the CMuD was mounted in self-coincidence. This was done by dividing the 9 WLS fibers by two SiPM's and coincide the their signals. In the third case a second CMuD was used test their coincidence characteristics.

5. CMUD CHARACTERIZATION

Some of the characteristics of the CMuD were determined using different setups. In the first setup the efficiency and purity of the CMuD were studied. These characteristics were also measured for a CMuD in self-coincidence and with two CMuD in coincidence.

5.1. CMuD

In this section it was studied the characteristics of the Compact Muon Detector.

5.1.1. Efficiency

The detector was biased with 67.25 V and the efficiency was measured. Each acquisition took around 24 hours in order to obtain large counts and minimize the error.

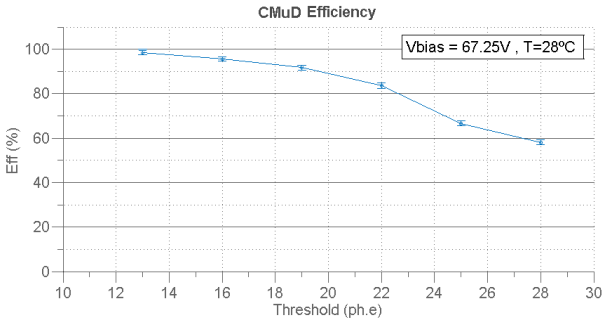

Figure 6: Plot of the CMuD efficiency in ph.e scale.

From this data it is possible to hint at that the minimum number of photoelectrons generated by a passing muon is close to 14-15 ph.e. For this thresholds the detection probability is almost 100%, which means that all muons are detected.

5.1.2. Purity

In this measurement a a flag was set in that stopped the acquisition when the number of events seen by the CMuD reached 260 000. The CMuD was biased at 67.25 V. The data acquired is plotted in figure 7.

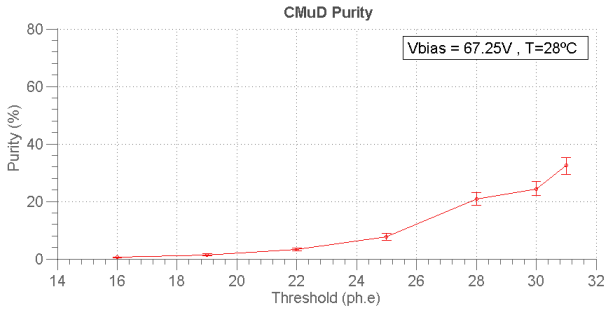

Figure 7: Plot of the efficiency in ph.e scale.

As it would be expected the higher the threshold the higher is the purity of the detector. This is a consequence to the decrease in the dark current rate. If the minimum number of ph.e. generated by a muon in the CMuD is around 15 ph.e, it would be desirable for the purity at that threshold to be high. Instead the purity seems to be very low at that threshold, only increasing for about ~ 28 ph.e.

5.2. CMuD in Self-Coincidence

In this setup the CMuD was placed in self-coincidence. This was achieved by dividing the 9 WLS fibers that make the detector into two different SiPM's. This means that there are two signals coming from the same detector. A coincidence of these two signals was performed and the resulting signal was taken as the output of the CMuD. It is important that the fibers are consecutively divided to the bottom and top circuit because the fibers that absorb more photons are the ones closer to the place where the muon crossed the scintillator. This division ensures that each those two fibers are always going to a different SiPM's. This helps to make the resulting two signals identical, which is essential if the intent is to create a coincidence.

Two different acquisitions were done: one where the fibers were divided by the the SiPM's has in figure **??** and another where the SiPM's were not connected to the detectors at all. The second measurement will give the dark rate of this setup. The difference between the two measurements should provide an insight about the signal the CMuD in self-coincidence generates.

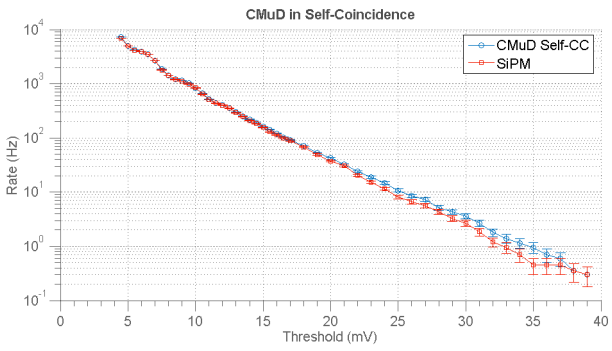

Figure 8: Signal of the CMuD in self-coincidence and respective dark current rate.

Even though the dark current rate is greatly reduced, the self-coincidence signal seems to never detach from it. This means that is likely that the signal produced by a muon is now too small to be separated from the noise

5.2.1. *Efficiency*

The results show a great decrease in the efficiency being only about 15% for 4 ph.e. threshold and rapidly decreasing to about 2%.

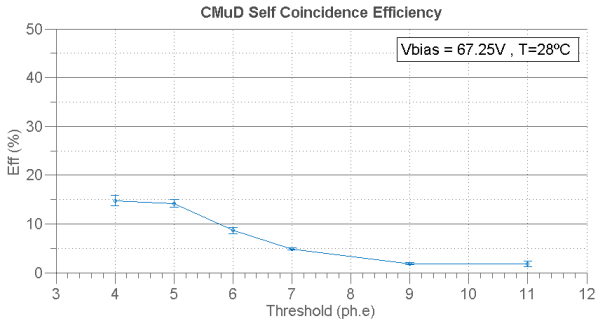

Figure 9: Plot of the efficiency in ph.e scale.

This can be explained by the division the signal goes through with the separation of the fibers by the SiPM's. According to the CMuD measurements (5.1), each muon generates 15 ph.e. If these photo-electrons were evenly originated from the two fibers closer to the path of the muon it is probable that the self-coincidence would work. Generating a signal of about 7-8 ph.e. ($\sim$ 25 mV) in each SiPM. But it seems likely that the signal generated is asymmetric thus creating a significantly higher signal in on SiPM and a lower in the other making it difficult see a coincidence at high thresholds.

5.2.2. *Purity*

By analyzing the self-coincidence signal (figure 8 it can be expected for the purity to be very low, since the signal basically coincides with the dark current. In any case the threshold was set to 8 ph.e. ($\sim$ 27 mV) an increased from there.

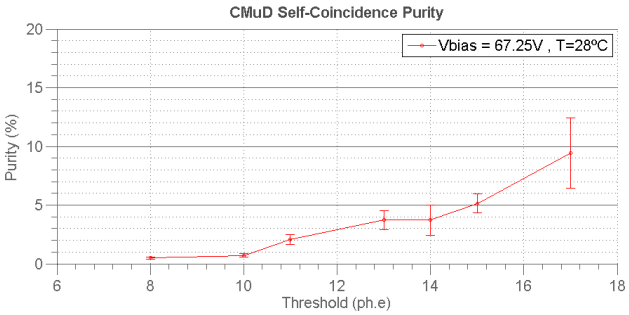

Figure 10: Plot of the efficiency in ph.e scale.

The measurement confirms the expectations with a very low purity even for relatively high thresholds where the dark current ratio is close to zero. The last data point shows such a big error because rate of events was so small that very few events were counted.

The results of the self-coincidence setup are not very good. This is because the signal generated by a muon appears to be lower than what was expected. This is probably because of the asymmetry of the signals that reach the photo-detectors.

5.3. Two CMuD's in Coincidence

In this section two CMuD's were setup in coincidence. With this setup it is possible to reduce the dark rate, similarly to the reduction in self-coincidence, while maintaining the signal generated by a muon in the CMuD. The coincidence signal was measured with the detectors vertically aligned and side by side. The difference between these measurements should correspond to the muon rate. The result is plotted in figure 11.

As was expected, the order of magnitude of the coincidence rate resembles the self-coincidence signal plotted in figure 8. However, unlike the self-coincidence measurement, there is a clear separation between the signal and the dark current at around 7 ph.e. ($\sim$ 23 mV). For higher thresholds the signal seems to maintain a stable value, of about , $R_\mu = 4$ Hz, while the dark current keeps decreasing. This plateau corresponds to the muon flux, R_μ, crossing the CMuD.

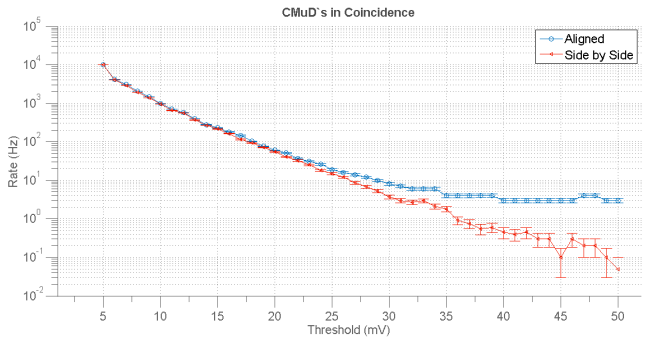

Figure 11: Measurement of two CMuD's in coincidence aligned and side by side.

5.3.1. *Efficiency*

The efficiency of two CMuD's in coincidence seems to stay constant for low thresholds, maintaining a value of about 80%. Around 15 ph.e the efficiency starts to steadily decrease. This behavior is similar to the one observed in the measurement of the CMuD efficiency, shown in figure 10. This seems to confirm that the minimum signal a muon generates in a CMuD is around 15 photo-electrons.

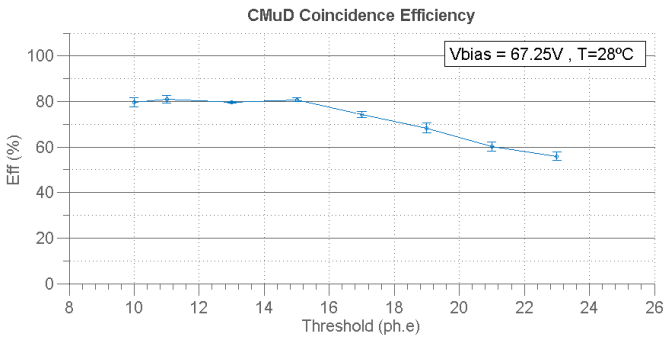

Figure 12: Plot of the detection efficiency of two CMuD's in coincidence in ph.e scale.

5.3.2. *Purity*

The purity measurements shows a great increase from the 10 ph.e. to the 13 ph.e threshold, going from around 50% to about 90% purity. This threshold range, corresponding to about 33-43 mV, seems to match the transition of the dark rate from a 1-2 hertz to about 0.2 Hz in the signal measurement in figure 11. In this transition the dark rate goes from having the same order of magnitude of the muon flux to being one order of magnitude lower. This explains the increase in purity observed. For thresholds higher than 13 ph.e, the purity remains stable value of about 98%.

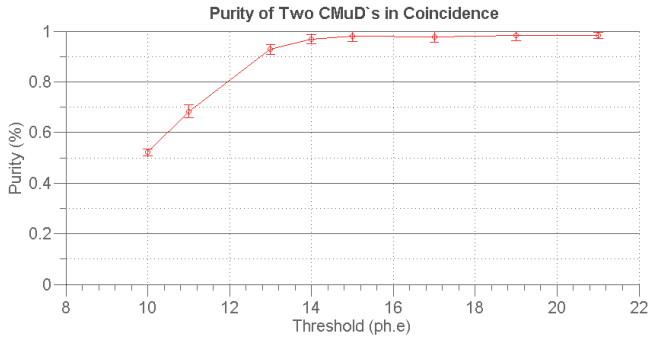

Figure 13: Plot of the purity in ph.e scale.

The data shows that two CMuD's in coincidence can produce a detector with a very high purity and efficiency. Comparing the plots of the efficiency, in figure 12 and purity, in figure 13, it is possible to determine that the threshold that maximizes the combination of these characteristics is between 14-15 ph.e.

6. CONCLUSION & OVERVIEW

In the first place the CMuD detector meet the requirements for this project. It is simple to setup, relatively cheap and safe. The tests performed on the CMuD prototype reviled a good detection efficiency. The data indicates that each muon generates a signal of at least 15 ph.e. The self-coincidence setup has shown fairly poor results either in the efficiency or purity. When two CMuD's were setup in coincidence it was possible to achieve a very good combination of efficiency/purity with its maximization happening when their plateaus coincidence - at 14-15 ph.e threshold.

In the future a DAQ card will be integrated to bias the detector and perform the amplification, discrimination and coincidence of the signal, replacing the experimental apparatus necessary this study. This will simplify the use of the detector and allow its distribution by local high schools for testing.

[1] R. Franke, M. Holler, B. Kaminsky, T. Karg, H. Prokoph, A. Schönwald, C. Schwerdt, A. Stößl, and M. Walter. Cosmo-a cosmic muon observer experiment for students. *arXiv preprint arXiv:1309.3391*, 2013.

[2] T. K. energy MeV and I. Mean excitation energy eV. 30. passage of particles through matter.

[3] E. Garutti. The physics particle detectors.

[4] P. N. Dinh, N. T. Dung, B. D. Hieu, P. T. Phuong, P. Darriulat, N. T. Thao, D. Q. Thieu, and V. Van Thuan. Measurement of the zenith angle distribution of the cosmic muon flux in hanoi. *Nuclear Physics B*, 661(1):3–16, 2003.